chemistry proceedings

MDPI

Proceeding Paper

Design and In Silico Profiling of Semi-Synthetic Abietane Diterpenoids with Promising Anticancer Activity †

Vera M. S. Isca [1], Rebeca André [1], Przemysław Sitarek [2], Anna Merecz-Sadowska [3,4], Magdalena Małecka [5], Monika Owczarek [6], Joanna Wieczfinska [7], Radosław Zajdel [3,8], Paweł Nowak [3], Tomasz KowalczyK [9] and Patricia Rijo [1,10,*]

[1] Center for Research in Biosciences & Health Technologies (CBIOS), Universidade Lusófona, 1749-024 Lisbon, Portugal; vera.isca@ulusofona.pt (V.M.S.I.); rebeca.andre@ulusofona.pt (R.A.)
[2] Department of Medical Biology, Medical University of Lodz, Muszynskiego 1, 90-151 Lodz, Poland; przemyslaw.sitarek@umed.lodz.pl
[3] Department of Economic and Medical Informatics, University of Lodz, 90-214 Lodz, Poland; anna.merecz-sadowska@uni.lodz.pl
[4] Department of Allergology and Respiratory Rehabilitation, Medical University of Lodz, 90-725 Lodz, Poland
[5] Department of Physical Chemistry, Faculty of Chemistry, University of Lodz, Pomorska 163/165, 90-236 Lodz, Poland; magdalena.malecka@chemia.uni.lodz.pl
[6] Łukasiewicz Research Network, Lodz Institute of Technology, Skłodowskiej-Curie 19/27, 90-570 Lodz, Poland; monika.owczarek@lit.lukasiewicz.gov.pl
[7] Department of Immunopathology, Medical University of Lodz, Zeligowskiego 7/9, 90-752 Lodz, Poland; joanna.wieczfinska@umed.lodz.pl
[8] Department of Medical Informatics and Statistics, Medical University of Lodz, 90-645 Lodz, Poland
[9] Department of Molecular Biotechnology and Genetics, Faculty of Biology and Environmental Protection, University of Lodz, Banacha 12/16, 90-237 Lodz, Poland; email@email.com
[10] Instituto de Investigação do Medicamento (iMed.ULisboa), Faculdade de Farmácia, Universidade de Lisboa, 1649-003 Lisbon, Portugal
* Correspondence: patricia.rijo@ulusofona.pt

† Presented at the 29th International Electronic Conference on Synthetic Organic Chemistry (ECSOC-29); Available online: https://sciforum.net/event/ecsoc-29.

Abstract

Diterpenoids belonging to the abietane class, including compounds like 7α-acetoxy-6β-hydroxyroyleanone (Roy) from *Plectranthus grandidentatus*, show strong anticancer potential. Semi-synthetic Roy derivatives were evaluated in silico for pharmacokinetics (ADMET), drug-likeness, and toxicity. PASS predicted high anticancer activity (scores 0.819–0.879), while DFT analysis revealed favorable electronic properties and reactivity. Molecular docking showed strong binding to oncogenic targets (CDKs, BCL-2, caspases, RTKs, p53), supported by stable interactions in MD simulations. Overall, the derivatives demonstrated promising pharmacological profiles and molecular stability, supporting their potential as anticancer agents and warranting further experimental validation.

Keywords: plectranthus; diterpenoids; anticancer activity; ADMET; DFT; molecular dynamics

Academic Editor(s): Name

Published: date

Citation: Isca, V.M.S.; André, R.; Sitarek, P.; Merecz-Sadowska, A.; Małecka, M.; Owczarek, M.; Wieczfinska, J.; Zajdel, R.; Nowak, P.; KowalczyK, T.; et al. Design and In Silico Profiling of Semi-Synthetic Abietane Diterpenoids with Promising Anticancer Activity. *Chem. Proc.* **2025**, *volume number*, x. https://doi.org/10.3390/xxxxx

1. Introduction

Cancer remains a major global health concern, with mortality rates projected to rise significantly. Conventional treatments like surgery and chemotherapy often fall short due to resistance and side effects, highlighting the need for new therapeutic approaches, especially those derived from natural sources [1,2].

Medicinal plants offer a rich resource of bioactive compounds with diverse pharmacological effects [3]. *Plectranthus* genus, part of the Lamiaceae family, includes hundreds of species used in traditional medicine for conditions ranging from infections to inflammation [4]. These plants are known for their phenolics and terpenoids, particularly abietane diterpenoids [5]. Studies have shown that Plectranthus extracts and isolated compounds possess antioxidant, antimicrobial, and anticancer properties [6]. Notably, acetone and methanolic extracts from *P. madagascariensis* and *P. neochilus* have demonstrated strong antibacterial and radical scavenging activity, as well as cytotoxic effects on breast cancer cells [7,8]. One such molecule, 7α-acetoxy-6β-hydroxyroyleanone (Roy, **1**, Figure 1), has shown promising activity and inspired the synthesis of related analogs for further evaluation [9,10].

Computational methods now play a key role in assessing these derivatives. Techniques like molecular docking, dynamics simulations, and network pharmacology help predict drug-likeness, toxicity, and protein interactions [11,12]. These in silico tools streamline the discovery of effective anticancer agents and guide future lab testing.

2. Results and Discussion

This study focused on evaluating the lead molecule Roy (compound **1**) along with ten newly synthesized derivatives, assessing their chemical properties through computational methods. The aim was to identify compounds with enhanced biological potential. By integrating experimental findings with in silico analysis, the work supports the development of promising candidates for therapeutic applications.

2.1. Compounds

Ten ester derivatives (**2–11**) of compound **1** were previously synthesized from Roy **1** and characterized through Fourier-transform infrared spectroscopy (FTIR), Nuclear Magnetic Resonance (NMR), and High-resolution mass spectrometry (HRMS) analysis [11,12].

Chemical structures of Roy (**1**) and new derivatives **2–11** are shown in Table 1.

2.2. ADMET and Drug-Likeness Analysis Results

To better understand the behavior and potential applications of the compounds, their physicochemical properties were evaluated using the SwissADME server. The selected compounds exhibited molecular weights between 348.43 and 634.66 g/mol, with compounds **2**, **3**, **6**, **7**, **8**, and **11** exceeding 500 g/mol.

Their lipophilicity values ranged from 2.31 to 6.40, and compounds **3**, **6**, and **11** showed values above 5, suggesting potential for oral bioavailability. Lipophilicity plays a crucial role in pharmacokinetic behavior and is a key parameter in the drug discovery process.

The screened compounds display a range of water solubility, ranging from moderate to poor solublility. Given their solubility profiles the screened compounds may require formulation strategies aimed at improving solubility.

Key pharmacokinetic predictions such as GI absorption, BBB permeability, Pgp substrate classification, and CYP inhibition profiles were assessed to evaluate the compounds' drug-likeness and safety. High gastrointestinal absorption was observed for most compounds except **6** and **12**. The blood–brain barrier (BBB) permeability potential, a key parameter for evaluating the ability of compounds to reach the central nervous system, was also assessed. All tested compounds were predicted to be potential substrates of P-glycoprotein (P-gp). Regarding cytochrome P450 (CYP) enzyme inhibition, compounds **2**, **5**, **7**,

8 and **11** were predicted to inhibit two CYP isoforms, while compounds **1**, **3**, **4**, **6**, **9**, and **10** showed inhibition of a single isoform.

Drug-likeness and lead-likeness profiles parameters were obtained by using the SwissADME server. Most of the compounds did not fully comply with at least one of the five commonly used filters (Lipinski, Ghose, Veber, Egan, and Muegge), with only Roy **1** meeting all criteria. he predicted bioavailability score for all compounds corresponded to a 56% probability class. Additionally, each compound triggered at least one PAINS or BRENK alert and showed a lead-likeness violation. More details on the physicochemical properties of the screened compounds can be consulted in Isca et al. [11] and Merecz-Sadowska et al. [12].

2.3. Antineoplastic and Anticarcinogenic Activity Results

Table 2 presents the predicted antineoplastic and anticarcinogenic activities of the tested compounds, as assessed using the PASS server. All compounds demonstrated a high probability of antineoplastic activity (Pa > 0.5). Comparative analysis of Pa and Pi values for anticarcinogenic potential indicated that compounds 1, 2, and 4 exceeded the 0.3 Pa threshold. Based on established criteria, compounds with Pa values above 0.3 are considered potentially bioactive [13]. More detail on the antineoplastic and anticarcinogenic activities of the screened compounds can be consulted in Isca et al. [11] and Merecz-Sadowska et al. [12].

2.4. Density Functional Theory Calculation Results

Frontier molecular orbitals, specifically the highest occupied molecular orbitals (HOMO) and lowest unoccupied molecular orbitals (LUMO), offer important insights into the reactivity and stability of the compounds. The conformations of compounds **1–11**, optimized using density functional theory (DFT), are presented in Table 3.

The energy of the LUMO reflects a molecule's capacity to accept electrons, whereas the HOMO energy indicates its potential to donate electrons [14]. A smaller HOMO–LUMO gap suggests greater susceptibility to polarization and typically more reactivity. Conversely, a wider HOMO–LUMO energy gap suggests that the molecule is less prone to polarization, as it requires more energy for electronic excitation [15]. For compounds **1–11**, HOMO–LUMO gaps ranged from 2.63 to 3.79 eV. Compound **3** showed the lowest gap, indicating the highest reactivity, as less energy is needed to excite the molecule from its ground state. Compound **11** had the widest gap, suggesting the lowest chemical reactivity among the series. Further information on molecular orbitals and related descriptors is available in the studies by Isca et al. [11] and Merecz-Sadowska et al. [12].

2.5. Molecular Docking Results

Molecular docking was performed to assess the interactions between all compounds (**1–11**) and ten cancer-related proteins including caspases 3 and 9, p53, BCL-2, BCL-XL, CDKs 2 and 6, PARP-1, EGFR, and VEGFR. These targets are key regulators of cell proliferation, survival, angiogenesis, and genomic stability in cancer pathways. This structure-based approach supports the identification of selective small-molecule candidates with potential anticancer activity. Structural evaluation using CAST-p confirmed the presence of well-defined active sites suitable for ligand interaction. The docking results revealed strong predicted affinities, with several compounds, particularly compounds **1**, **3**, **6**, **7**, **9**, **10**, and **11**, exhibiting highly favorable binding energies with one or more of the target proteins under investigation. Benchmarking against known inhibitors validated the docking protocol and highlighted the potential of the screened compounds to match or exceed the binding performance of established drugs. Detailed discussions of molecular docking can be found in Isca et al. [11] and Merecz-Sadowska et al. [12].

As illustrative examples, the binding poses and interactions of compounds **1**, **5**, and **10** are visually represented in Figure 2, highlighting typical ligand–protein docking behavior observed across the dataset. Overall, the favorable docking outcomes for compounds **1** (caspase 9, (**A**) in Figure 2), **5** (BCL-2 (**B**), CDK2 (**C**), EGFR (**D**) and VEGFR (**E**)), **3** (caspase 3, PARP-1and CDK6), **6** (BCL-XL, p53 and caspase 9), **7** (BCL-2), **9** (EGFR (**F**), BCL-XL (**G**), caspase 3 (**H**), CDK2 (**I**), VEGFR (**J**), and p53 (**K**) in Figure 2) suggest that these molecules may serve as potent inhibitors of the therapeutically relevant protein targets.

2.6. Molecular Dynamics Simulation Results

To assess the dynamic behavior of the docking complexes, molecular dynamics (MD) simulations were performed over a 100 ns timescale. These simulations aimed to evaluate the stability of protein–ligand interactions by analyzing the root-mean-square deviation (RMSD) values. The RMSD profiles for the protein backbones stabilized within a range of 2.4 Å to 3.4 Å, indicating that the systems reached equilibrium without significant conformational drift. Ligand RMSD values remained consistently low, mostly below 0.3 nm, after the initial 60 ns, suggesting that the ligands remained securely bound within the active site. Further information is available in the studies by Isca et al. [11] and Merecz-Sadowska et al. [12]. These results confirm the robustness of the docking poses and the dynamic stability of the interactions, supporting the potential of the screened compounds for further development.

3. Materials and Methods

3.1. Plant Material

Plant material from *Plectranthus grandidentatus* Gürke, previously studied and sourced from the Parque Botânico da Tapada da Ajuda (ISA, Lisbon), originated from cuttings obtained at Kirstenbosch National Botanical Garden (Cape Town, South Africa). A voucher specimen (841/2007) is deposited at the João de Carvalho e Vasconcellos Herbarium. The material, collected between 2007 and 2008, was dried and stored under controlled conditions. Taxonomic identity was confirmed via the World Flora Online database (accessed 31 May 2023). (http://www.worldfloraonline.org/, accessed on 31 May 31 2023).

3.2. Extraction and Isolation

Dried aerial parts of *P. grandidentatus* were extracted with acetone using an ultrasound-assisted method, as described in a previous study [10]. The process involved three 30-minute sonication cycles, followed by filtration and vacuum evaporation at 40 °C, yielding 2.3% (w/w). The crude extract was then fractionated chromatographically. Compound **1** (7α-acetoxy-6β-hydroxyroyleanone, Roy) was isolated as yellow crystals by recrystallization from *n*-hexane, and its structure matched previously reported data.[16].

*3.3. Semi-Synthesis of Derivatives of Compound **1***

Esterification was performed according to the optimized procedure described by Isca et al. method [10]. These compounds were originally synthesized in studies by Isca et al. [11], Merecz-Sadowska et al. [12], Bessa et al. [17] and Garcia et al. [18].

3.4. ADMET and Drug-Likeness Analysis

The ADMET profiles and drug-likeness of the compounds were previously described by Isca et al. [11] and Merecz-Sadowska et al. [12]

3.5. Anticarcinogenic Activity

The anticancer potential of the compounds was predicted using the PASS server (http://www.pharmaexpert.ru/passonline/, accessed on 25 October 2023). Activity was expressed as probable activity (Pa) and probable inactivity (Pi), with Pa > Pi indicating promising candidates for biological validation. [19].

3.6. DFT Calculations

Ligand 3D structures were built in Avogadro v1.95 and converted to XYZ format. DFT calculations were performed in ORCA v5.03 using B3LYP functional and Def2-TZVPP basis set under gas-phase conditions [20]. Results were analyzed in Avogadro [21].

3.7. Molecular Docking and Molecular dynamics

Molecular docking and MD simulations of selected ligand–protein complexes were conducted following approaches previously described by Isca et al. [11] and Merecz-Sadowska et al. [12].

3.8. Figures, Tables and Schemes

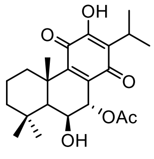

1

Figure 1. 7α-acetoxy-6β-hydroxyroyleanone (Roy) **1**.

Table 1. 7α-acetoxy-6β-hydroxyroyleanone (Roy) **1** and its semi-synthetic derivatives (**2**–**11**).

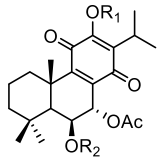

1

Derivative	R_1	R_2	Derivative	R_1	R_2
2	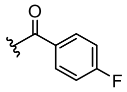	H	**7**	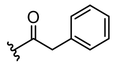	H
3	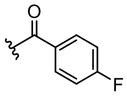	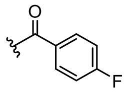	**8**	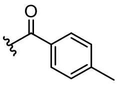	H
4	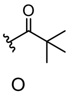	H	**9**	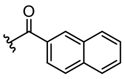	H
5	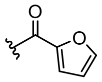	H	**10**	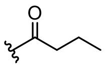	H
6	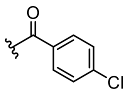	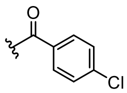	**11**	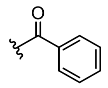	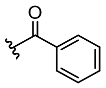

Table 2. Predicted antineoplastic and anticarcinogenic activity of the examined compounds obtained by using the PASS server.

Compounds	Antineoplastic Activity		Anticarcinogenic Activity	
	Pa Value	Pi Value	Pa Value	Pi Value
1	0.879	0.005	0.419	0.028

2	0.810	0.010	0.315	0.053
3	0.822	0.009	0.279	0.067
4	0.882	0.0005	0.312	0.054
5	0.770	0.016	0.255	0.080
6	0.811	0.010	0.289	0.063
7	0.810	0.010	0.315	0.053
8	0.822	0.009	0.279	0.067
9	0.882	0.0005	0.312	0.054
10	0.770	0.016	0.255	0.080
11	0.811	0.010	0.289	0.063

Table 3. HOMO-LUMO diagram of compounds **1–11**.

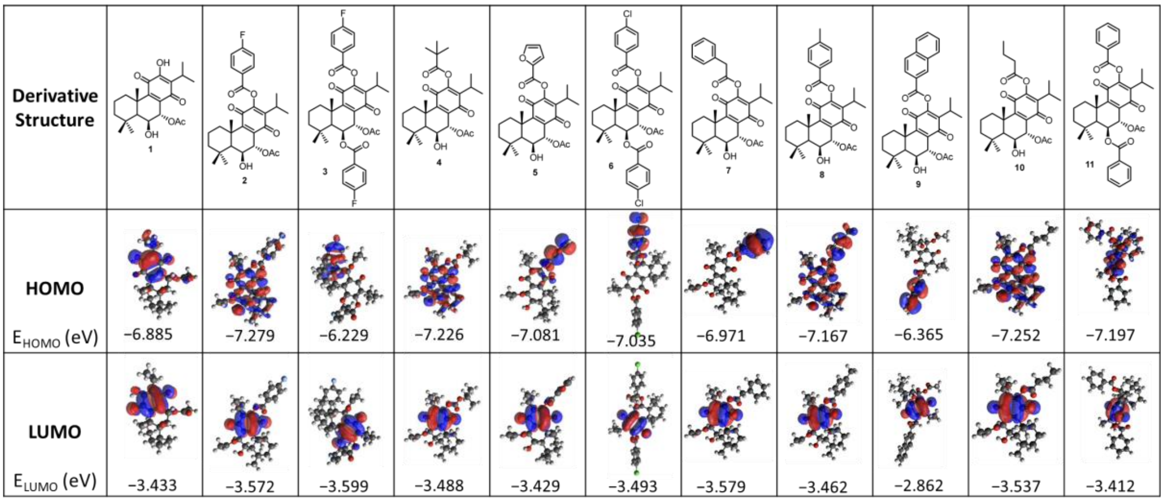

Derivative Structure	1	2	3	4	5	6	7	8	9	10	11
HOMO E_{HOMO} (eV)	−6.885	−7.279	−6.229	−7.226	−7.081	−7.035	−6.971	−7.167	−6.365	−7.252	−7.197
LUMO E_{LUMO} (eV)	−3.433	−3.572	−3.599	−3.488	−3.429	−3.493	−3.579	−3.462	−2.862	−3.537	−3.412

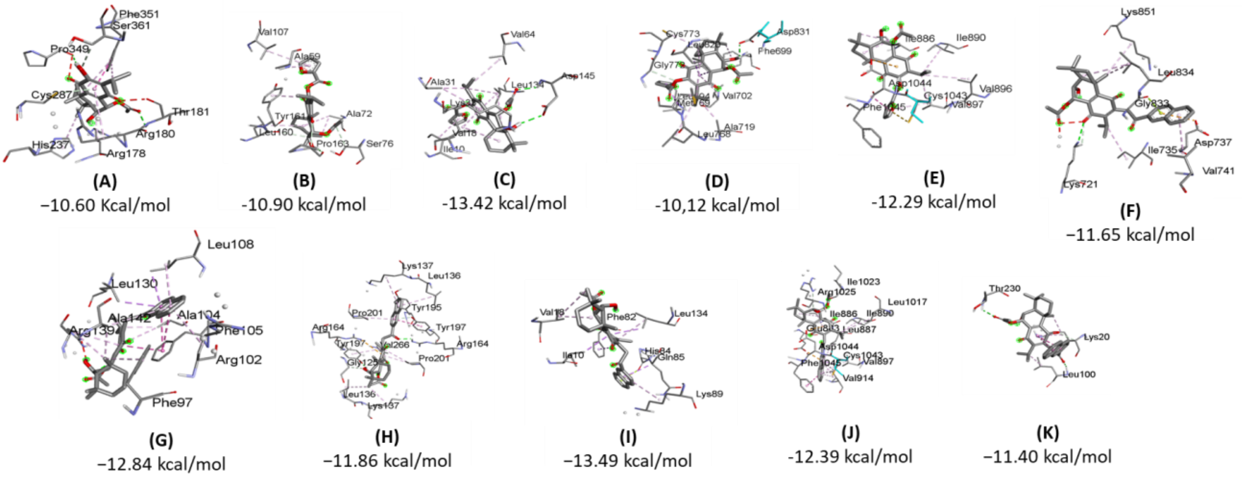

(A) −10.60 Kcal/mol

(B) −10.90 kcal/mol

(C) -13.42 kcal/mol

(D) −10,12 kcal/mol

(E) -12.29 kcal/mol

(F) −11.65 kcal/mol

(G) −12.84 kcal/mol

(H) −11.86 kcal/mol

(I) −13.49 kcal/mol

(J) -12.39 kcal/mol

(K) -11.40 kcal/mol

Figure 2. Interaction between compounds (**1**, **5** and **9**) and the active sites of target proteins implicated in cancer-related pathways. 3D interactions and binding energy of compound **1** against caspase 9 (**A**); compound **5** against BCL-2 (**B**), CDK2 (**C**), EGFR (**D**) and VEGFR (**E**); and compound **10** against EGFR (**F**), BCL-XL (**G**), caspase 3 (**H**), CDK2 (**I**), VEGFR (**J**), and p53 (**K**).

5. Conclusions

The integrated approach used in the study, combining physicochemical profiling, quantum chemical calculations, and molecular modeling enabled the efficient screening of a focused library of Roy derivatives. The compounds display promising pharmacological profiles and are predicted to interact with key pathways involved in cancer cell proliferation, survival, and genomic stability. Structural modifications appear to enhance these properties relative to the parent compound. Collectively, computational findings offer a strong rationale for further experimental validation through in vitro studies, supporting their continued development as potential anticancer agents.

Author Contributions: Conceptualization, A.M-S., P.S., and R.Z.; methodology, M.M., M.J., V.I., P.R., and K.Z.; software, A.M-S, P.S., T.K., K.Z. and M.J.; validation, M.M., M.J. V.I., P.R., and K.Z.; formal analysis, H.Z-B and R.Z.; investigation, A.M-S., M.M., P.S, T.K., V.I. and P.R.; data curation, H.Z-B., A.M-S.; writing—original draft preparation, A.M-S, P.S., V.I. and P.R.; writing—review and editing, T.K., M.M., K.Z., H.Z-B, M.J. and R.Z.; visualization, A.M-S., K.Z. and M.J; supervision, A.M-S. and R.Z; project administration, R.Z. and A.M-S.; funding acquisition, R.Z. All authors have read and agreed to the published version of the manuscript.

Funding: This research received no external funding.

Institutional Review Board Statement: Not applicable.

Informed Consent Statement: Not applicable.

Data Availability Statement: Not applicable.

Acknowledgments: This work was supported by FCT (Portugal) through the projects with reference DOI 10.54499/UIDP/04567/2020 and DOI 10.54499/UIDB/04567/2020 and the PhD grant (SFRH/BD/137671/2018).

Conflicts of Interest: The authors declare no conflicts of interest.

References

1. Brennan, P.; Davey-Smith, G. Identifying Novel Causes of Cancers to Enhance Cancer Prevention: New Strategies Are Needed. *JNCI: J. Natl. Cancer Inst.* **2022**, *114*, 353–360. https://doi.org/10.1093/jnci/djab204.
2. Mattiuzzi, C.; Lippi, G. Current Cancer Epidemiology. *J. Epidemiol. Glob. Health* **2019**, *9*, 217–222.
3. Elshafie, H.S.; Camele, I.; Mohamed, A.A. A Comprehensive Review on the Biological, Agricultural and Pharmaceutical Properties of Secondary Metabolites Based-Plant Origin. *Int. J. Mol. Sci.* **2023**, *24*, 3266. https://doi.org/10.3390/ijms24043266.
4. Lukhoba, C.W.; Simmonds, M.S.J.; Paton, A.J. Plectranthus: A Review of Ethnobotanical Uses. *J. Ethnopharmacol.* **2006**, *103*, 1–24. https://doi.org/10.1016/j.jep.2005.09.011.
5. Ladeiras, D.; M. Monteiro, C.; Pereira, F.; P. Reis, C.; A. M. Afonso, C.; Rijo, P. Reactivity of Diterpenoid Quinones: Royleanones. *Curr. Pharm. Des.* **2016**, *22*, 1682–1714. https://doi.org/10.2174/1381612822666151211094521.
6. Gáborová, M.; Šmejkal, K.; Kubínová, R. Abietane Diterpenes of the Genus Plectranthus Sensu Lato. *Molecules* **2022**, *27*, 166. https://doi.org/10.3390/molecules27010166.
7. Pereira, M.; Matias, D.; Pereira, F.; P. Reis, C.; Simões, M.F.; Rijo, P. Antimicrobial Screening of Plectranthus Madagascariensis and P. Neochilus Extracts. *J. Biomed. Biopharm. Res.* **2015**, *12*, 127–138. https://doi.org/10.19277/BBR.12.1.111.
8. Matias, D.; Nicolai, M.; Fernandes, A.S.; Saraiva, N.; Almeida, J.; Saraiva, L.; Faustino, C.; Díaz-Lanza, A.M.; Reis, C.P.; Rijo, P.; et al. Comparison Study of Different Extracts of Plectranthus Madagascariensis, P. Neochilus and the Rare P. Porcatus (Lamiaceae): Chemical Characterization, Antioxidant, Antimicrobial and Cytotoxic Activities. *Biomolecules* **2019**, *9*, 179. https://doi.org/10.3390/biom9050179.
9. Śliwiński, T.; Sitarek, P.; Skała, E.; Isca, V.M.S.; Synowiec, E.; Kowalczyk, T.; Bijak, M.; Rijo, P. Diterpenoids from Plectranthus Spp. As Potential Chemotherapeutic Agents via Apoptosis. *Pharmaceuticals* **2020**, *13*, 123. https://doi.org/10.3390/ph13060123.

10. Isca, V.M.S.; Bangay, G.; Princiotto, S.; Saraíva, L.; dos Santos, D.J.V.A.; García-Sosa, A.T.; Rijo, P. Extraction Optimization and Reactivity of 7α-Acetoxy-6β-Hydroxyroyleanone and Ability of Its Derivatives to Modulate PKC Isoforms. *Sci. Rep.* **2024**, *14*, 16990. https://doi.org/10.1038/s41598-024-67384-0.
11. Isca, V.M.S.; Sitarek, P.; Merecz-Sadowska, A.; Małecka, M.; Owczarek, M.; Wieczfińska, J.; Zajdel, R.; Nowak, P.; Rijo, P.; Kowalczyk, T. Anticancer Effects of Abietane Diterpene 7α-Acetoxy-6β-Hydroxyroyleanone from Plectranthus Grandidentatus and Its Semi-Synthetic Analogs: An In Silico Computational Approach. *Molecules* **2024**, *29*, 1807. https://doi.org/10.3390/molecules29081807.
12. Merecz-Sadowska, A.; Isca, V.M.S.; Sitarek, P.; Kowalczyk, T.; Małecka, M.; Zajdel, K.; Zielińska-Bliźniewska, H.; Jęcek, M.; Rijo, P.; Zajdel, R. Exploring the Anticancer Potential of Semisynthetic Derivatives of 7α-Acetoxy-6β-Hydroxyroyleanone from Plectranthus Sp.: An In Silico Approach. *Int. J. Mol. Sci.* **2024**, *25*, 4529. https://doi.org/10.3390/ijms25084529.
13. Filimonov, D.A.; Lagunin, A.A.; Gloriozova, T.A.; Rudik, A. V; Druzhilovskii, D.S.; Pogodin, P. V; Poroikov, V. V Prediction of the Biological Activity Spectra of Organic Compounds Using the PASS Online Web Resource. *Chem. Heterocycl. Compd.* **2014**, *50*, 444–457.
14. Yu, J.; Su, N.Q.; Yang, W. Describing Chemical Reactivity with Frontier Molecular Orbitalets. *JACS Au* **2022**, *2*, 1383–1394.
15. Huang, Y.; Rong, C.; Zhang, R.; Liu, S. Evaluating Frontier Orbital Energy and HOMO/LUMO Gap with Descriptors from Density Functional Reactivity Theory. *J. Mol. Model.* **2017**, *23*, 3.
16. Isca, V.M.S.; Sencanski, M.; Filipovic, N.; Dos Santos, D.J.V.A.; Čipak Gašparović, A.; Saraíva, L.; Afonso, C.A.M.; Rijo, P.; García-Sosa, A.T.; Santos, D.; et al. Activity to Breast Cancer Cell Lines of Different Malignancy and Predicted Interaction with Protein Kinase C Isoforms of Royleanones. *Int. J. Mol. Sci.* **2020**, *21*, 367. https://doi.org/10.3390/ijms21103671.
17. Bessa, C.; Loureiro, J.B.; Barros, M.; Isca, V.M.S.; Sardão, V.A.; Oliveira, P.J.; Bernardino, R.L.; Herman-de-Sousa, C.; Costa, M.A.; Correia-de-Sá, P.; et al. Counteracting Colon Cancer by Inhibiting Mitochondrial Respiration and Glycolysis with a Selective PKCδ Activator. *Int. J. Mol. Sci.* **2023**, *24*, 5710. https://doi.org/10.3390/ijms24065710.
18. Garcia, C.; Isca, V.M.S.; Pereira, F.; Monteiro, C.M.; Ntungwe, E.; Sousa, F.; Dinic, J.; Holmstedt, S.; Roberto, A.; Díaz-Lanza, A.; et al. Royleanone Derivatives From Plectranthus Spp. as a Novel Class of P-Glycoprotein Inhibitors. *Front. Pharmacol.* **2020**, *11*, 1711.
19. Lagunin, A.; Stepanchikova, A.; Filimonov, D.; Poroikov, V. PASS: Prediction of Activity Spectra for Biologically Active Substances. *Bioinformatics* **2000**, *16*, 747–748.
20. Neese, F.; Wennmohs, F.; Becker, U.; Riplinger, C. The ORCA Quantum Chemistry Program Package. *J. Chem. Phys.* **2020**, *152*.
21. Hanwell, M.D.; Curtis, D.E.; Lonie, D.C.; Vandermeersch, T.; Zurek, E.; Hutchison, G.R. Avogadro: An Advanced Semantic Chemical Editor, Visualization, and Analysis Platform. *J. Cheminform* **2012**, *4*, 17.